JOURNAL OF MATERIALS SCIENCE 26 (1991) 1327–1332

Invariant three- and four-phase equilibria in the magnesium-rich corner of the Mg–Cu–Sn ternary system

E. E. VICENTE*, S. BERMÚDEZ*, A. ESTEBAN‡, R. TENDLER*
*Departamento de Materiales and ‡División Tecnología de Plutonio, Comisión Nacional de Energía Atómica, Av. Libertador 8250, 1429 Buenos Aires, Argentina

B. ARCONDO, H. SIRKIN
Departamento de Física, Facultad de Ingeniería, Universidad de Buenos Aires, Paseo Colón 850, 1063 Buenos Aires, Argentina

Invariant three- and four-phase equilibria in the magnesium-rich corner of the Mg–Cu–Sn ternary system have been studied by differential thermal analysis, optical microscopy, electron probe microanalysis and X-ray diffraction. The $L \leftrightharpoons (Mg) + Mg_2Cu + Mg_2Sn$ ternary eutectic reaction was found to be at 467 °C and at Mg–13.5 at % Cu–4.4 at % Sn. The $L \leftrightharpoons Mg_2Cu + Mg_2Sn$ pseudo-binary eutectic reaction is tentatively located at 522 °C and at Mg–26.0 at % Cu–7.7 at % Sn.

1. Introduction

Magnesium-rich alloys of the Mg–Cu–Sn system have been shown to be quite suitable for the development of experimental and theoretical thermodynamic studies on the glass-forming ability of ternary alloys [1, 2]. More specifically, the Mg–Mg_2Cu–Mg_2Sn [3] ternary sub-system has a phase diagram that is rather simple: it is made up by the Mg–Mg_2Cu [4] and Mg–Mg_2Sn [5] binary sub-systems, and by the Mg_2Cu–Mg_2Sn [3] pseudo-binary sub-system. The melting point of magnesium is 650 °C [6]. Mg_2Cu and Mg_2Sn stoichiometric intermetallic compounds melt congruently at 568 and 770.5 °C, respectively. The Mg–Mg_2Cu sub-system has a eutectic point at 14.5 at % Cu and 485 °C. The solubility of copper in magnesium is very low: 0.013 at % Cu at 485 °C. The Mg–Mg_2Sn sub-system has a eutectic point at 10.7 at % Sn and 561.2 °C. The maximum solubility of tin in magnesium is 3.35 at % Sn at 561.2 °C [4, 5].

However, the information available on the ternary system is insufficient to give details concerning the liquidus valleys and the four-phase equilibria. For instance, the pseudo-binary eutectic point $L \rightleftharpoons Mg_2Cu + Mg_2Sn$, actually a saddle point in the ternary system, is suggested to be located at 525 °C and at Mg–25.6 at % Cu–7.7 at % Sn. The system is also reported to exhibit a ternary eutectic point $L \rightleftharpoons (Mg) + Mg_2Cu + Mg_2Sn$, which has been provisionally located at Mg–11.4 at % Cu–3.2 at % Sn, but its temperature has not been measured [3]. (Mg) stands for the terminal solid solution. The above values of composition have been estimated from the published phase diagram [3].

In this work we have measured the composition and the temperature of both the ternary and the pseudo-binary eutectic reactions.

2. Experimental procedure

Two alloys of the following nominal compositions were prepared: (A) Mg–11.4 at % Cu–3.2 at % Sn and (B) Mg–25.6 at % Cu–8.0 at % Sn. Starting materials were magnesium, copper and tin of 99.99% purity. The alloys (A: 0.5099 g and B: 0.6679 g) were melted at 800 °C during 30 min in nuclear-grade graphite crucibles ($\approx$ 1 g each) in an electric resistance furnace under a static argon atmosphere ($\approx$ 3 atm) of 99.998% purity. A weight loss of 5.43% for alloy A and 1.08% for alloy B was observed.

Simultaneous differential thermal analysis (DTA) and thermogravimetry (TG) were performed in Mettler Vacuum Thermoanalyzer equipment, under a static argon atmosphere ($\approx$ 1 atm) of 99.998% purity, and in the same crucibles which had been previously used for the preparation of the alloys. An empty graphite crucible was chosen as the reference "sample". The heating/cooling rates were: 6 °C min^{-1} (25 to 436 °C) and 1 °C min^{-1} (436 to 500 °C) for alloy A, and 6 °C min^{-1} (25 to 507 °C) and 1 °C min^{-1} (507 to 556 °C) for alloy B. After the last measurement in each alloy they were heated up to 507 °C (alloy A) and 557 °C (alloy B). Next, the furnace of the DTA–TG equipment was turned off and the samples were allowed to cool inside the furnace down to room temperature at a rate of about 6 °C min^{-1}. Weight losses of the crucibles containing the alloys during the DTA–TG experiments were negligible ($\approx$ 0.01%). The Pt/Pt–10% Rh thermocouple was calibrated *in situ* against high-purity 99.995% indium, 99.99% aluminium and silver, and 99.999% tin and zinc.

The solidification structures, after the DTA–TG experiments, were examined by optical microscopy in cross-sections at the top, centre and bottom of the ingots. The specimens were prepared for microscopic

0022–2461/91 $03.00 + .12

examination by grinding without any lubricant on a Buheler microcut paper sheet (600 grit soft), followed by mechanical polishing on a Mol–Struers cloth with 3 μm diamond paste lubricated with ethylene glycol. The samples were then chemically etched by immersion, stirring for 6 sec in a solution of picric acid, ethanol and water (6 g:10 ml:90 ml). Finally, they were washed and rinsed with anhydrous ethanol (water was specially avoided to prevent oxidation).

The phases were identified by their colours under the light microscope and by electron probe microanalysis (EPMA) in Cameca SX 50 equipment outfitted with a wavelength-dispersive spectrometer. In order to improve the accuracy of the composition measurements, the specimens for EPMA were polished but unetched. In spite of the fact that the samples were unetched, very good secondary electron images were achieved. The phases were also identified by X-ray diffraction (XRD) in Philips PW 1400 equipment employing graphite-monochromatized Co$K\alpha$ radiation.

3. Results

Both alloys show off-eutectic microstructures (Figs 1 to 6 below). The bottom of alloy A has elongated colonies of the (Mg)–Mg_2Cu binary eutectic in a fine background matrix of the (Mg)–Mg_2Cu–Mg_2Sn ternary eutectic (Fig. 1). Towards the top of the ingot non-faceted, primary dendrites of (Mg) were also observed (Fig. 2). Primary (Mg) certainly segregated upwards by gravity during the freezing of this alloy. The morphology of the binary eutectic is nearly lamellar and that of the ternary one seems to be fibrous or rod-like, both Mg_2Cu and Mg_2Sn compounds being partially surrounded by (Mg) (Fig. 3). The interlamellar spacing of the binary eutectic ranges between 5 and 10 μm, and the inter-rod spacing of the ternary eutectic is approximately 2 μm.

12 measurements of composition performed by EPMA on 15 μm × 15 μm scanned areas on the finest ternary eutectic zones resulted in the following average value: Mg–13.5 at % Cu–4.4 at % Sn, which is slightly different from the one reported previously [3]. Standard deviations in composition were: 0.5 at % Mg, 0.4 at % Cu and 0.3 at % Sn. EPMA performed in five different dendrites of (Mg) gave an average composition of Mg–1.5 at % Sn–0.05 at % Cu. The thermogram of this alloy (Fig. 7 below) shows only one peak at 467 °C, as measured on the initial deviation from the baseline [7] during both melting and solidification, which is attributable to the ternary eutectic reaction. No primary arrest was observed.

Sample B exhibits a honeycomb pattern of colonies (sometimes termed "grains") of the Mg_2Cu–Mg_2Sn pseudo-binary eutectic (Fig. 4). The size of the cells ranges between 100 and 500 μm. This eutectic has a mixed lamellar–rodlike morphology, Mg_2Cu being the major phase (Fig. 5). The size of the inter-rod or interlamellar spacing is about 1 to 2 μm at the centre of the colonies. In addition, the specimen has very few, isolated, faceted, primary crystals of Mg_2Sn, and also small amounts of an intercellular, three-phase assemblage that resembles a ternary eutectic (Fig. 6). It includes Mg_2Cu, Mg_2Sn and a reddish third phase (as viewed on unetched metallographic surfaces), this colour indicating the presence of a higher copper content.

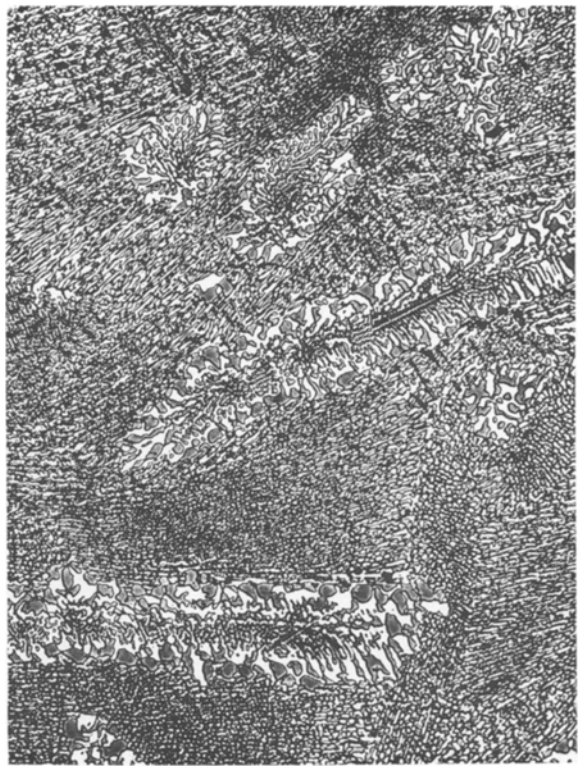

Figure 1 Optical micrograph of alloy A, as-cast. Colonies of the (Mg)–Mg_2Cu binary eutectic in a matrix of the (Mg)–Mg_2Cu–Mg_2Sn ternary eutectic. (Mg): grey, Mg_2Cu: white, Mg_2Sn: black. Magnification 200 × .

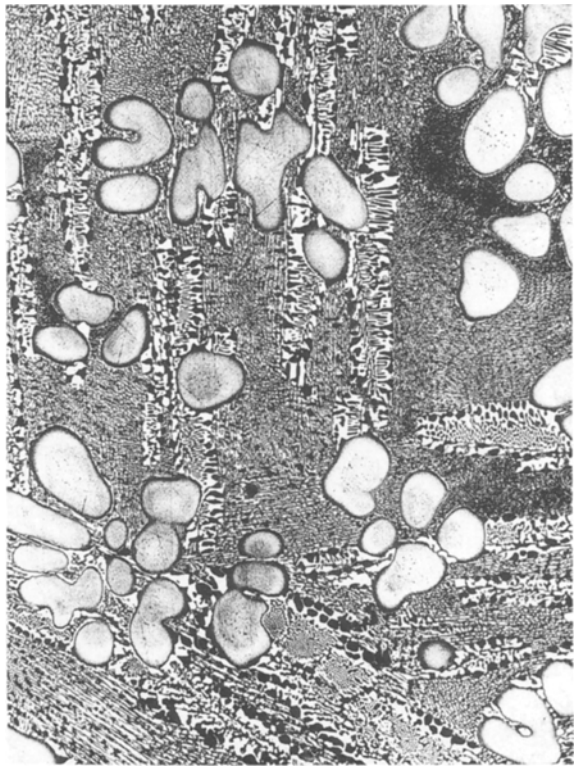

Figure 2 As Fig. 1. Zone showing primary dendrites of (Mg). Magnification 100 × .

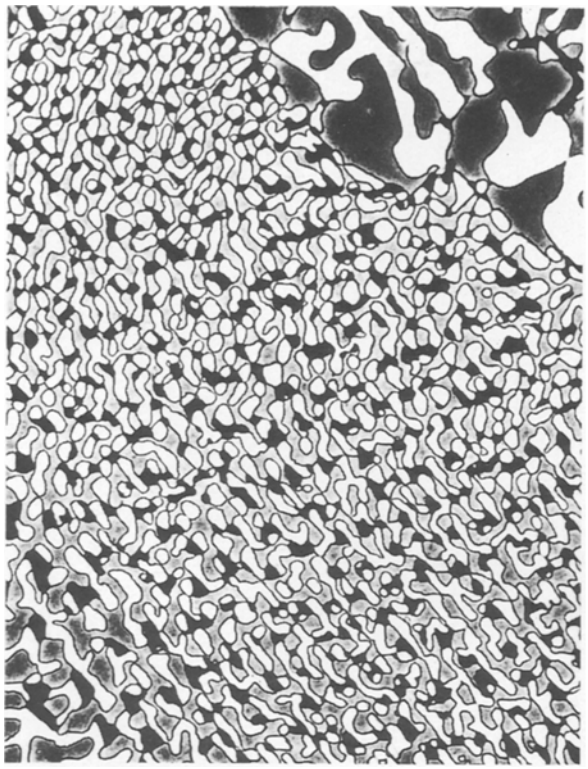

Figure 3 As Fig. 1. Magnification 1000 × .

Figure 5 As Fig. 4. Magnification 1000 × .

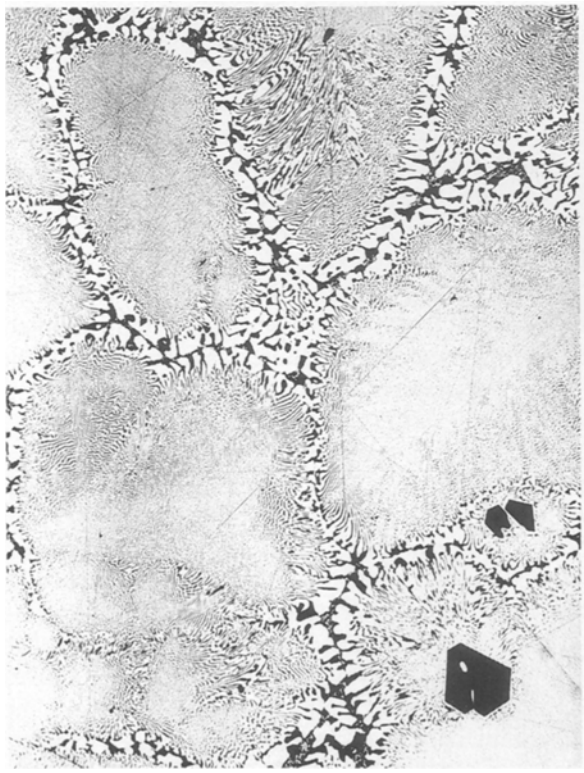

Figure 4 Optical micrograph of alloy B, as-cast. Colonies of the Mg_2Cu–Mg_2Sn pseudo-binary eutectic, and primary crystals of Mg_2Sn. Mg_2Cu: white, Mg_2Sn: black. Magnification 120 × .

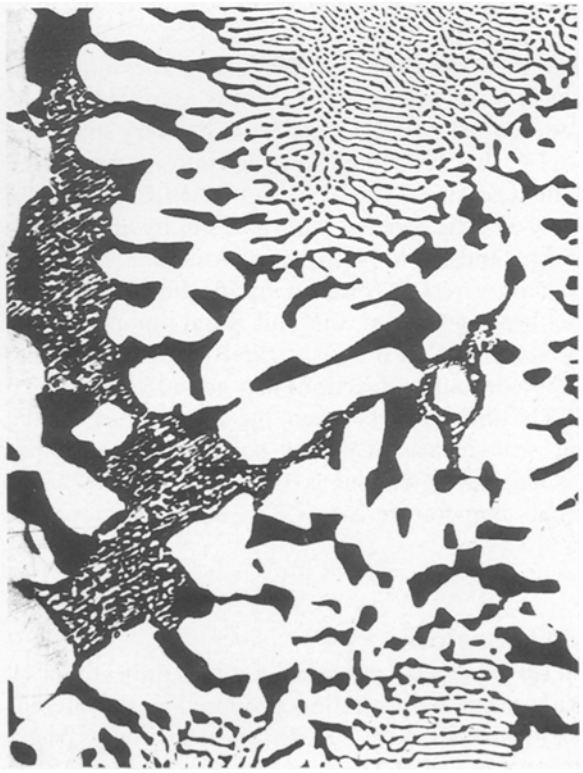

Figure 6 As Fig. 4. Zone showing intercellular three-phase assemblage. Mg_2Cu: white, Mg_2Sn: black, copper-rich phase: grey. Magnification 570 × .

The average composition of this assemblage could not be suitably measured by EPMA. The XRD pattern shows the existence of only Mg_2Cu and Mg_2Sn phases. The copper-rich phase could not be detected by XRD because there is only a small percentage of it in the whole sample. Six measurements of composition carried out by EPMA on 15 μm × 15 μm scanned areas on the finest pseudo-binary eutectic regions resulted in the following average value: Mg–26.0 at % Cu–7.7 at % Sn, which closely agrees with that

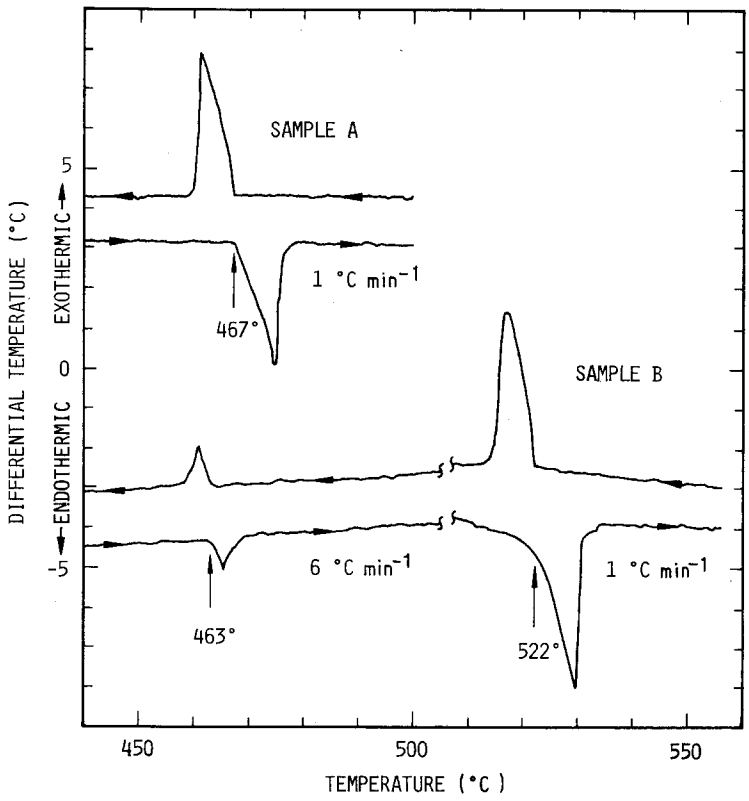

Figure 7 Thermograms of alloys A and B.

reported previously [3]. Standard deviations in composition were: 0.1 at % Mg, 0.2 at % Cu and 0.07 at % Sn.

The thermogram of this alloy (Fig. 7) exhibits two peaks: a large one at 522 °C that is ascribable to the pseudo-binary eutectic reaction, and a very small one at 463°C that could not be assigned to any reported invariant reaction. The $L \rightleftharpoons (Mg) + Mg_2Cu + Mg_2Sn$ ternary eutectic reaction was ruled out by both metallography and DTA. No primary arrest was observed. The main arrest is rounded by the beginning point upon heating and at the end point upon cooling, suggesting that an invariant three-phase equilibrium (the pseudo-binary reaction) was not strictly attained [7]. The difference between the temperature of the main peak measured during solidification and that measured during melting is 0.5 °C. The pseudo-binary eutectic temperature is just 3 °C below the reported value [3].

4. Discussion

Both the previously published liquidus projection [3], and the liquidus projection proposed in the present work for the Mg–Mg_2Cu–Mg_2Sn ternary sub-system, are shown in Fig. 8. The last one was plotted using the assessed binary phase diagrams [4, 5], the pseudo-binary eutectic point reported previously [3] and the ternary eutectic point measured in this work. Because of the lack of data, the field boundaries, which are the eutectic valleys, have been tentatively drawn as straight lines.

The weight losses that occurred on melting alloys A and B have to be mainly attributed to the vaporization of magnesium, because this is the volatile component [8]. On account of these magnesium losses, the corrected compositions become Mg–12.2 at % Cu–3.5 at % Sn for alloy A, and Mg–26.1 at % Cu–8.1 at % Sn for alloy B (points A′ and B′, respectively, in Fig. 8).

The observed microstructure of sample A and its corrected composition lack consistency [9] if the last is located on the previously estimated phase diagram [3]. Instead, the microstructure is consistent with the corrected composition when this is placed on the phase diagram proposed in this work. In fact, the alloy A′ lies within the primary phase field of (Mg) of the phase diagram proposed here, and within the angle delimited by the Mg–Cu binary system and by the straight line joining the magnesium corner and the (Mg)–Mg_2Cu–Mg_2Sn ternary eutectic point (Fig. 8). The solidification path [10, 11] of this alloy is quite simple. On cooling from the melt, initial crystallization of primary (Mg) occurs at some unknown liquidus temperature. Primary arrest in the thermogram of sample A is absent, probably because its liquidus temperature is above 500 °C. Let us assume that pure magnesium instead of (Mg) precipitates. The composition of its complementary liquid then moves along the extension of line Mg–A′ away from the magnesium corner. When the Mg–Mg_2Cu eutectic valley is reached ($467\,°C < T < 485\,°C$) this eutectic begins to solidify. From this point the composition of the liquid runs along this eutectic valley towards the Mg–Mg_2Cu–Mg_2Sn ternary eutectic point. The crystallization ends at the quaternary invariant point E (467 °C), where the remainder of the liquid isothermally transforms into the ternary eutectic.

Because (Mg) instead of pure magnesium is actually the primary phase, the first step of the solidification path is not a straight line but a curve. There are not enough data on the solubility of tin and copper in

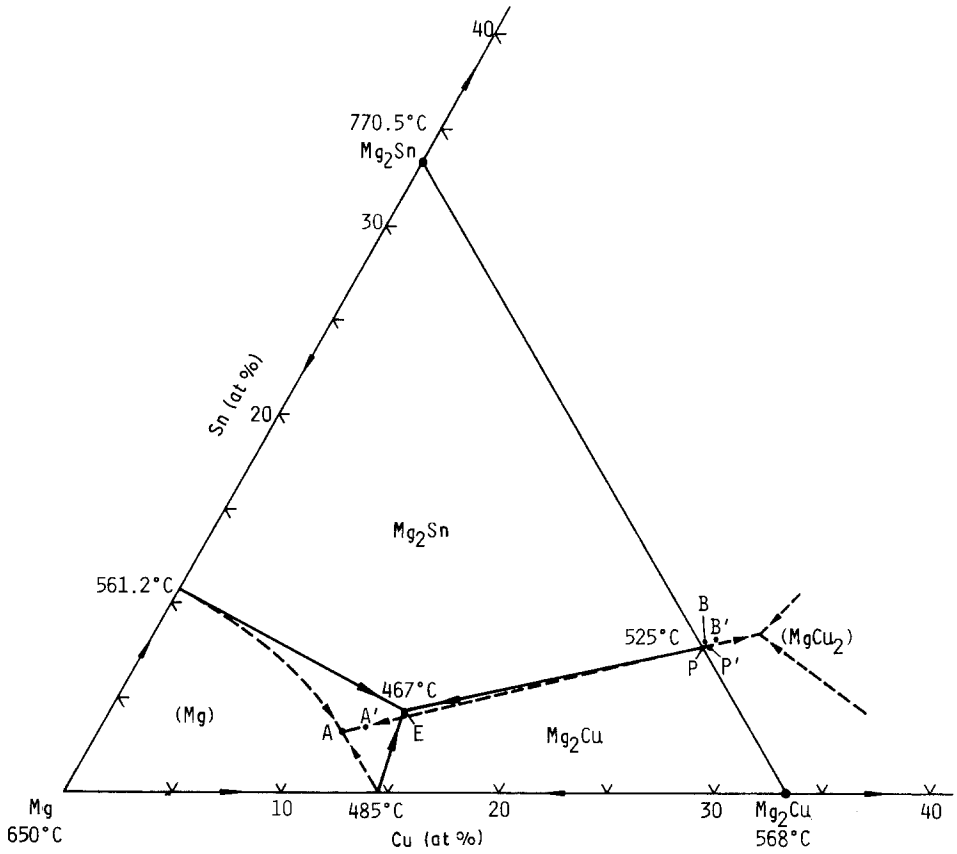

Figure 8 Liquidus projection of the Mg–Mg_2Cu–Mg_2Sn ternary sub-system: (– – –), Chang *et al.* [3], (——) this work. A and A′ are the nominal and the corrected compositions of alloy A, respectively. A and E are the reported [3] and measured (this work) composition of the ternary eutectic, respectively. B and B′ are the nominal and corrected compositions of alloy B, respectively. P and P′ are the reported [3] and measured (this work) compositions of the pseudo-binary eutectic, respectively.

(Mg), except a rough estimation at 400 °C [3]. However, from the binary phase diagrams [4, 5] and from our measurements of composition in primary (Mg), we can state that tin is more soluble in (Mg) than is copper. In addition, the solubility of tin in (Mg) decreases from 2.4 at % at 500 °C to 1.8 at % at 465 °C for Mg–Sn binary alloys [5]. Therefore, the first step of the solidification path of sample A should be slightly convex (as viewed from the Mg–Cu binary system), but it will certainly run towards the (Mg)–Mg_2Cu eutectic valley. The equilibrium reactions that occurred upon cooling of sample A can be summarized as follows:

$$L \rightarrow L + (Mg) \rightarrow L + (Mg) + Mg_2Cu \rightarrow (Mg) + Mg_2Cu + Mg_2Sn$$

Both the nominal and the corrected composition of sample B lie within the primary phase field of Mg_2Sn, very close to the Mg_2Cu–Mg_2Sn field boundary, but slightly shifted from the pseudo-binary section towards the $(MgCu_2)$–Mg_2Cu–Mg_2Sn ternary sub-system proposed previously [3]. $(MgCu_2)$ stands for the solid solution of copper, magnesium and tin in $MgCu_2$. Thus, the equilibrium reactions that occurred upon cooling of sample B could be summarized as follows:

$$L \rightarrow L + Mg_2Sn \rightarrow L + Mg_2Sn + Mg_2Cu \rightarrow Mg_2Sn + Mg_2Cu + (MgCu_2)$$

The microstructure of sample B is consistent with such reactions. However, the solidification path for the alloy B′, for instance, should end at the $L \rightarrow (MgCu_2) + Mg_2Cu + Mg_2Sn$ ternary eutectic point, tentatively located at Mg–27.8 at % Cu–8.4 at % Sn and 520 °C [3]. The small arrest at 463 °C measured in the thermogram of sample B suggests a different temperature for this ternary eutectic reaction, or the existence of some other non-reported invariant reaction. On the other hand, for Mg–Cu and Mg–Sn binary systems the liquidus lines show no discontinuities at the congruent points of Mg_2Cu and Mg_2Sn intermetallic compounds, but they form maxima with horizontal tangents and hence they are mathematically continuous. Likewise, the liquidus surfaces of the ternary system show no discontinuities when they cross the pseudo-binary cut [12]. Furthermore, the field boundary which is the intersection of two liquidus surfaces ($L + Mg_2Cu$ and $L + Mg_2Sn$) has a horizontal tangent (a maximum temperature of equilibrium among these three phases at the saddle point) [10].

These considerations permit us to state that the temperature of the pseudo-binary eutectic reaction measured in this work should be slightly below the "true" temperature of the saddle point. Hence, the results presented in Fig. 8 are provisional and more careful experiments are needed to establish this region of the phase diagram.

5. Conclusions

The $L \rightleftharpoons (Mg) + Mg_2Cu + Mg_2Sn$ ternary eutectic reaction was found to be at 467 °C and Mg–13.5 at % Cu–4.4 at % Sn. The $L \rightleftharpoons Mg_2Cu + Mg_2Sn$ pseudo-binary eutectic reaction is tentatively located at 522 °C and Mg–26.0 at % Cu–7.7 at % Sn.

Acknowledgements

The authors are grateful to Dr J. P. Abriata for stimulus and discussions, to Dr G. Vigna for leading the performance and interpretation of EPMA, and to Mr R. Gonzalez for performing the EPMA.

References

1. H. SIRKIN, N. MINGOLO, E. NASSIF and B. ARCONDO, *J. Non-Cryst. Solids* **93** (1987) 323.
2. F. SOMMER, M. FRIPAN and B. PREDEL, in Proceedings of 4th International Conference on Rapidly Quenched Metals, Sendai (Japan), August 1981, edited by T. Masumoto and K. Suzuki (Japan Institute of Metals, Sendai, 1982) p. 209.
3. Y. A. CHANG, J. P. NEUMANN, A. MIKULA and D. GOLDLANG, National Standard Reference Data System (National Bureau of Standards, USA, 1979) p. 520.
4. A. A. NAYEB-HASHEMI and J. B. CLARK, *Bull. Alloys Phase Diag.* **5** (1984) 36 and 103.
5. A. A. NAYEB-HASHEMI and J. B. CLARK, *ibid.* **5** (1984) 466 and 535.
6. "Melting point of the elements", *ibid.* **7** (1986) 601.
7. R. D. SHULL, *ibid.* **4** (1983) 5.
8. "Vapour pressure of the elements", in "Handbook of Chemistry and Physics", edited by R. C. Weast (CRC, Florida, 1978) p. D-258.
9. D. G. MacCARTNEY, J. D. HUNT and R. M. JORDAN, *Metall. Trans.* **11A** (1980) 1243.
10. F. N. RHINES, "Phase Diagrams in Metallurgy" (McGraw-Hill, New York, 1956) pp. 159 and 163.
11. A. D. PELTON, in "Physical Metallurgy", edited by R. W. Cahn and P. Haasen (Elsevier, Amsterdam, 1983) p. 327.
12. G. MASSING, "Ternary Systems" (Reinhold, New York, 1944) p. 42.

Received 16 January
and accepted 29 March 1990